Modeling of Isometric Muscle Properties via Controllable Nonlinear Spring, and Hybrid Model of Proprioceptive Receptors

Mario Spirito

Modeling of Isometric Muscle Properties via Controllable Nonlinear Spring, and Hybrid Model of Proprioceptive Receptors

Mario Spirito[a,]

[a]DEI - University of Bologna, Bologna, Italy

Abstract

We present a macroscopic anatomical behaviour of skeletal muscles. According to the data available in the literature, we propose a first model for the muscle isometric force generation depending on the muscle length and neuronal excitation frequency. We moreover provide a more physical-inspired model of the isometric force exploiting a nonlinear spring description with controllable characteristics, such as stiffness and rest length. Then, a hybrid model is proposed to describe the sensory system that provides the Central Nervous System (CNS) with the measurements of muscle length and its rate of change.

Keywords: Hybrid dynamical modelling, isometric force of muscle, nonlinear springs, proprioceptive receptors

1. Introduction

Skeletal muscles, or simply muscles, are organs of the muscular system whose cells have the characteristic to produce force and movements. They are mostly attached to the bones of the skeleton by tendons, and thanks to their contractile and elastic properties they allow the relative motion of the bones of the involved articulations. Thus, the controlled contraction of the muscles allows for the performance of everyday movements.

Each skeletal muscle consists of thousands of muscle fibers wrapped together by connective tissue sheaths, see Fig.1. The individual bundles of muscle fibers in a skeletal muscle are known as fasciculi. Each muscle fiber is comprised of several myofibrils containing many myofilaments. When bundled together, all the myofibrils get arranged in a unique striated pattern forming sarcomeres which are the fundamental contractile unit of a skeletal muscle. The two most significant myofilaments are actin and myosin filaments which are arranged distinctively to form various bands on the skeletal muscle [1][Ch.1], [2] and [3].

Skeletal muscles show up with neuronal innervations from the sensory-motor system. A set of neurons, the α-motoneurons, constitutes the neuromuscular junction and are responsible, according to their excitation frequency α measured in pulses per second, for sarcomeres contractions. And hence they allow the generation of the muscle active force. On the other hand, another set of neurons, constituting the proprioceptive receptors, carries from the muscle to the CNS the values of muscle length and rate of change (Ia- and II- Spindles), and the measurement of the force value at the tendon level (Ib-Spindle or Golgi Tendon Organs (GTO)).

We can thus see the muscle complex, from a 'System Engineering' standpoint, as a complex Multi-Input Multi-Output system with the actuator (α- motoneurons), the plant (the muscles cells, whose contraction produces the exerted force on the joint), and the sensors (Ia- and II- Spindles and GTO), and the CNS as a feedback controller. In Fig.2 a schematics of the involved connections in reported.

The modelling of how muscles exert force started with the work of Hill [5] in which the muscle description via a spring-like behaviour is presented. In particular, the relationship takes into account a contractile element that produces muscles force and this is in series to a passive element representing the tendon model between the muscles fibers and the connected bones. This model has then been exploited to generate more detailed models [6, 7] in which they describe the microscopic behaviour of contraction behaviour due to the effects of sarcomeres and cross-bridge. In [8], Hill's model has been enlarged by adding a 'damping element'. In [9, 10, 11], experimental data has been exploited to construct an analytic expression of the total force generated by the muscles. In these works, the total force has been split into length-dependent force F_L and a velocity-dependent force F_V, both depending on the α-motoneuron excitation frequency. The F_L term is then split, similarly to Hill's model, into an active plus passive term. The active force describes the part of fibers contraction when excited and produces movements, while the passive force only refers to the elastic mechanical behaviour of the muscle fibers.

Experimental data and models of isometric (fixed muscle length) and isokinetic (fixed muscle velocity) forces are available and presented in [9, 10, 11, 12, 13].

A system engineering perspective of the neuromuscular system has been presented in [8, 14, 15] in which they give a control-oriented interpretation of the involved parts. In [16] we find a work dealing with the optimal co-activation problem while optimizing the mechanical impedance of an antagonist actuated biological joint (such as an elbow). On the other hand, in [17] the authors aim at answering how much reduced the

Email address: mario.spirito3@unibo.it (Mario Spirito)

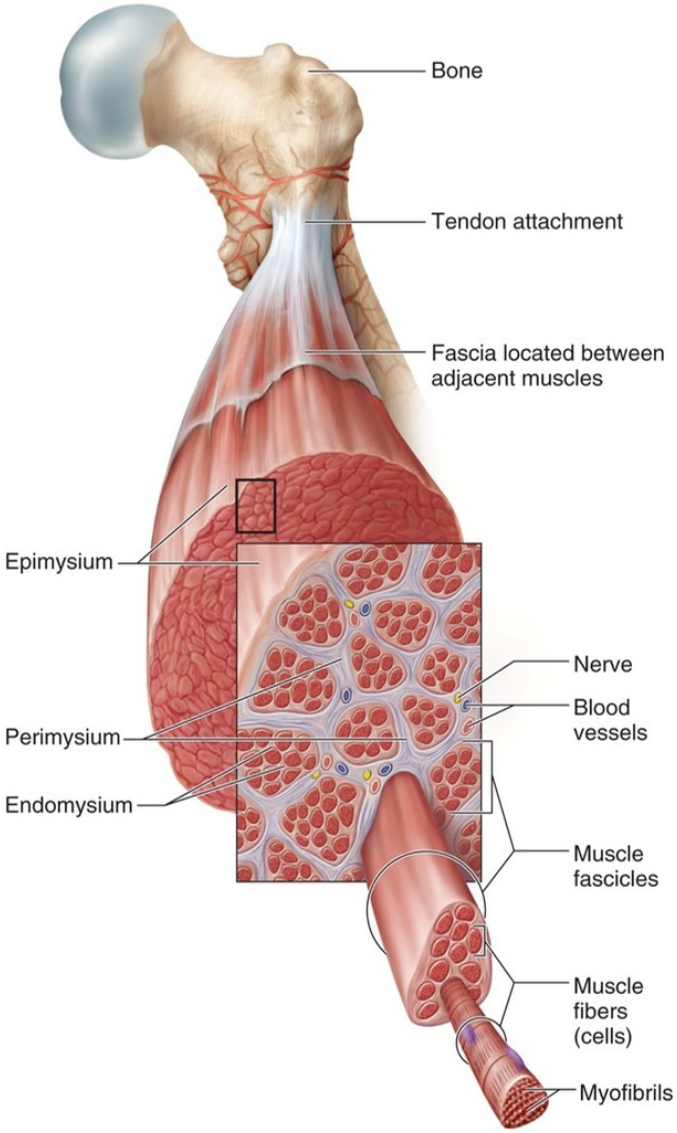

Figure 1: Muscle structure.

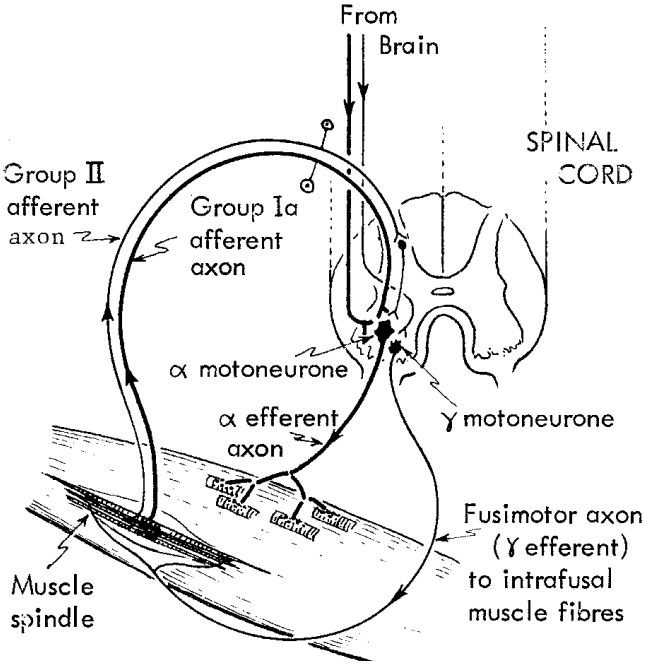

Figure 2: Muscle and Central Nervous System schematics of the connections. Picture taken from [4].

muscle model must be to be able to describe the neuromuscular system. In recent years, with the development of the contraction theory in the control field, the contractile properties of the neuromuscular system (involving Hill's model equations) have been studied in [18]. In [19] an analytic model of complete and incomplete tetanus contraction has been proposed, and so far, according to the authors' knowledge, gives the closest to reality, although incomplete, dynamical model of the muscle behaviour.

The sensory part involved in the muscle system is related to the measurement of the plant variables, such as force at the tendon level (GTO), and muscle/fibres length and velocity (Ia- and II-spindles). In the last century, they have been studied in depth [4, 20] and the most important works have been collected in [21], see [22] for a more recent review on the topic. From a system engineering perspective, the GTOs dynamical model has been proposed in [23] by exploiting a proper transfer function between the force exerted on the tendons and the GTO neurons' firing frequency. For Spindles Ia and II, in [24], a static model has been proposed to describe the relationship among the muscle/fibres length, velocity, and the γ-motoneurons excitation to the spindles firing rate. Such γ-motoneurons are in charge of modulating the firing responses of the connected Spindle system.

To the best of the authors' knowledge, there is no dynamical model of the Spindles organs available in the literature.

The sensory part plays an important role in the movement control architecture. In particular, the presence of internal loops between the muscles and the spinal cord allows the possibility to actuate the reflexes [15, 25, 26], such as: stretch reflexes, reciprocal inhibition, and others. The spinal cord, in this setup, is in between the CNS and α-motoneurons via the interneuron and it is unavoidably involved in movement control [27, 28, 29].

The paper is organized as follows, after having provided motivations for the work, in Section 2 we give some authors' considerations about the available data. We give in section3 an overview of the most relevant models available in the literature. Then, in section 4 we describe the developed models for the isometric muscle force. Eventually, before the conclusions in sec.6, we provide in sec.5 a hybrid modelling of the sensory system available in the muscles.

1.1. Motivations

This work aims to describe neuromuscular behaviour in a control theory paradigm. In particular, we would like to better understand the purposes of the neuromuscular loops and how they are exploited in controlling limbs movements, see for example [30] for the application of a stabilizing PID action on a single-link biomechanical model or [31] to see how this available measurement feedback can be exploited in position and

movement control. The reader can furthermore see [18] to have an insight on how waveform signals can be used to control delayed closed-loop systems, thus mimicking the spiking behaviour of biological nervous systems.

We strongly believe that this modelling idea would be a good starting point to eventually comprehend the purposes of the brain parts involved in the learning and control tasks of dexterous movements, see for example [32, 33, 34, 35, 36] to have a physiological and a biomechanical point of view of brain parts involved in movements control.

The final objective will then be to have a complete picture and understanding of the structure used by the brain in controlling human dexterous movements and thus mimic such a strategy in the field of nonlinear control systems such as nonlinear output regulation as in [37]. The study interleaves with the concept of inverse and forward models introduced, in neuroscience, by Wolpert and Kawato in their works [38, 39], see also [40] for another application of these models. So an intermediate step of the study will be to better understand how these models are formed, learned, and updated in the brain and how they are involved in the control strategy.

2. Preliminaries on available experimental data in literature

In the muscle force, we can distinguish among three main components: a passive force F_p that is always present due to the natural behaviour of tissues and only depends on the muscle length, we then have the active static (isometric) force F_L only depending on the muscle contraction (length L) and an active dynamic (eccentric and concentric) force F_V also depending on the rate of change of muscle contraction $\dot{L}$. The last two components are active terms and indeed they depend on the activation frequency α of the α-motoneuron.

Data of isometric force available in literature are mainly those in the figures of [10], [11], and [16], reported in this section for completeness. It is worth to notice that such data only

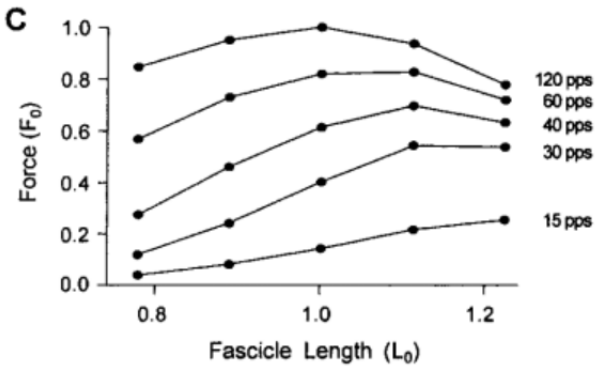

Figure 3: Normalized Isometric Force. Relationship between the static Force and the muscle length at different activation frequency. Plot taken from [11].

span the activation frequency in the interval $[0,120]$ pps (pulse per second), because 120 pps is the maximum excitation frequency the α-motoneuron can 'apply' on the muscle fibre.

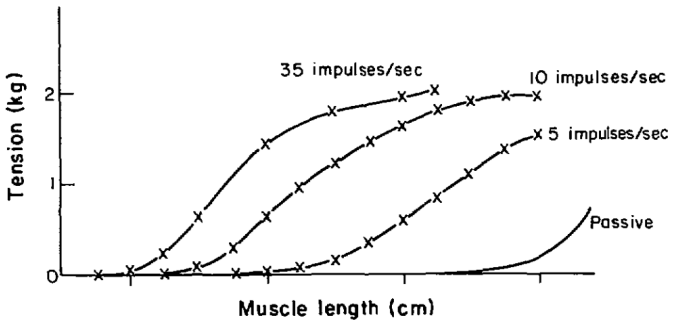

Figure 4: Isometric Force. Relationship between the static Force and the muscle length at different activation frequency. This plot is half useful due to the unknown length, but we can notice that there are different rest length (length at which the force is null) depending on the activation frequency. Plot taken from [16].

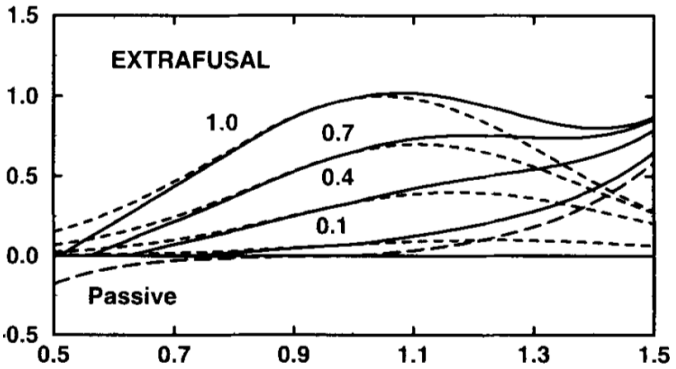

Figure 5: Normalized Isometric Force model with correction term given by a negative passive force in [10]. Here the activation frequency is normalized with respect to its maximum value $\alpha = 120$ pps

At $\alpha = 120$pps the active force F_L (i.e. the total force without passive F_p and dynamics F_V terms) has a maximum value indexed in literature by the symbol F_o. This maximum value F_o is associated to a specific length value L_o (which is not the maximum length value, but the length L corresponding to the maximum force value F_o at the maximum excitation frequency $\alpha = 120$pps). Almost all available data and proposed models in the literature are normalized with respect to these two values. Indeed we find force and length data of the form F/F_o and L/L_o, respectively. Due to this fact, we also consider a normalized model for such normalized values.

A crucial point in our model development is the presence in the force characteristic of rest length values (i.e. values of L for which the exerted force is null) that depends on excitation rates α, see Fig.4. And this fact leads us to consider a rest length function L_0 (which is not L_o as above) depending only on the excitation frequency α and this might be used to describe the contracting behaviour of the muscle. A major problem is that most of the data available in the literature lack these rest-length data which is fundamental for our model development. We thus exploit the same technique introduced in [10]. In practice, they first consider a model without the presence of rest length (based

on Gaussian terms, as it will be clearer at the end of section 3), and then they propose to add a negative passive term to compensate for the lack of rest lengths values in the model and obtain the rest lengths points saturating the force at zero. The approach is very clear in Fig. 5.

In the next section, we provide an overview of the two models available in the literature.

3. Literature models comparison

In our opinion, the most relevant and complete models in the literature are those available in [11] and [10]. Here we give a short description of such models for the sake of completeness.

3.1. Brown's et al model

In [11], as the Hill's model [5], the authors consider both the active isometric and the dynamic forces generators gathered inside a *contractile element* F_{CE} along which passive term F_{PE} describes the passive force (previously indicated as F_p, but we decided to stay faithful to the original nomenclature). The resulting total force F_{TOT} presents as

$$F_{TOT} = F_{CE} + F_{PE} \tag{1}$$

and F_{CE} is expressed as

$$F_{CE}(\alpha, L, \dot{L}) = R(\alpha)A(\alpha, L)F_L(L)F_V(L, \dot{L}) \tag{2}$$

where R is a fibre recruitment percentage and describes the amount of fibre involved in the force generation depending on the activation frequency, A is the term relating the muscle activation to the excitation frequency α and it would have values between 0 and 1 (the same values range has been considered for R), F_L and F_V describe respectively the force-length relationship and the force-velocity, and their product provides the force expression of the muscle depending on the current length L, the velocity of contraction $\dot{L}$, and excitation frequency α.

In their work, a simplified version of the force function is provided fixing $R(\alpha) = 1$ and making assumptions of quasi-statics (close to isometric) conditions during motion and of a starting length equal to the rest length, they hence move to a force expression of the type:

$$F_{CE}(\alpha, L, \dot{L}) = A_F(\alpha, L)\Big(F_L(L)F_V(L, \dot{L}) + F_p(L)\Big) \tag{3}$$

where

$$\begin{aligned}
A_f(\alpha, L) &= 1 - exp\left(-\left(\frac{\alpha}{0.56N_f(L)}\right)\right) \\
N_f(L) &= 2.11 + 4.16\Big(\frac{1}{L} - 1\Big) \\
F_L(L) &= exp\left(-\left|\frac{L^{1.93} - 1}{1.03}\right|^{1.87}\right) \\
F_p(L) &= -0.02e^{13.8 - 18.7L} \\
F_V(L, \dot{L}) &= \begin{cases} \frac{-5.72 - \dot{L}}{-5.72 + (1.38 + 2.09L)\dot{L}}, & \dot{L} \leq 0 \\ \frac{2.5 + 4.21L + 2.67L^2}{0.62 + \dot{L}}\dot{L}, & \dot{L} > 0 \end{cases}
\end{aligned} \tag{4}$$

In this model, one can notice that the length F_L and velocity F_V dependent force terms are multiplied one each other. This might lead to the interpretation that the velocity terms F_V are only acting as scaling functions on the 'supporting' isometric force F_L. We rather prefer to split the isometric F_L and dynamics F_V terms to analyse their contribution individually in a spring-damper fashion. Moreover, notice that when $\dot{L} \to 0^+$ in the equation we have $F_V \neq 1$, thus the model loses the continuity with the static isometric properties of the muscle after a lengthening phase.

3.2. Winters' Model

In [10], Winters work goes deep inside the basic muscle elements. Indeed in its work, we can find a microscopic description of the muscles components such as intrafusal and extrafusal elements with their relative damping and stiffness terms, and these are connected in parallel and series fashion. Of their work, we only focus on the isometric force that has been modelled as

$$F_{ISO}(\alpha, L_{CE}) = F_L(\alpha, L_{CE}) + F_p(L_{CE})$$

where, for the isometric force model, they exploit a Gaussian function with variable mean value

$$F_L(\alpha, L_{CE}) = \alpha e^{-\left(\frac{\frac{L_{CE}}{L_{m0}} - 1.05 - (1-\alpha)0.2}{0.4}\right)^2} \tag{5}$$

where L_{m0}, in Winter's notation, is the optimal muscle length value L_o (in this work notation), $L_{CE} = L_{mt} - L_{t0} - x_{SE}(L_{m0} + L_{t0})$ and x_{SE} is the (dimensionless) extension of the extrafusal series of spring-element, L_{mt} is the overall musculotendinous length and L_to is the tendon rest length. The value of α is normalized with respect to its maximum value. The passive force is instead given by the expression

$$F_{passive} = \begin{cases} \frac{e^{\frac{3}{0.6}\left(\frac{L_{CE}}{L_{m0}} - 1\right)} - 1}{e^3 - 1}, & \frac{L_{CE}}{L_{m0}} \geq 1 \\ -\frac{e^{\frac{6}{0.7}\left(1 - \frac{L_{CE}}{L_{m0}}\right)} - 1}{e^6 - 1}, & \frac{L_{CE}}{L_{m0}} < 1 \end{cases} \tag{6}$$

Notice that, as touched above, the passive force has a negative term for $\frac{L_{CE}}{L_{m0}} < 1$.

We strongly believe that, for our study purposes, the functions exploited in the models presented in this section are very complicated to manipulate and use in control analysis. Moreover, the parameters meaning is very difficult to interpret from a physical point of view.

4. Proposed Models

Our main objective is to describe the isometric force $(F_L + F_p)$ as a nonlinear controlled spring with variable stiffness K and rest length L_0

$$F_{ISO}(\alpha, L) = K(\alpha, L)\,(L - L_0(\alpha)) \tag{7}$$

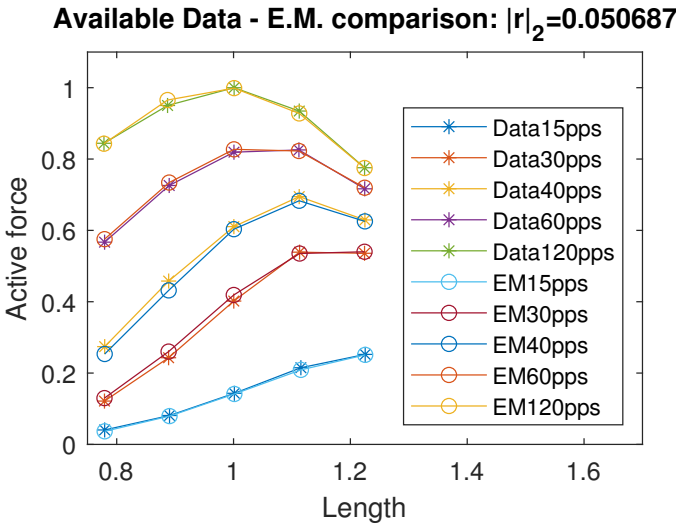

Figure 6: Data comparison between the available data in [11] and the evaluation/intermediate model. r indicates the residuals vector.

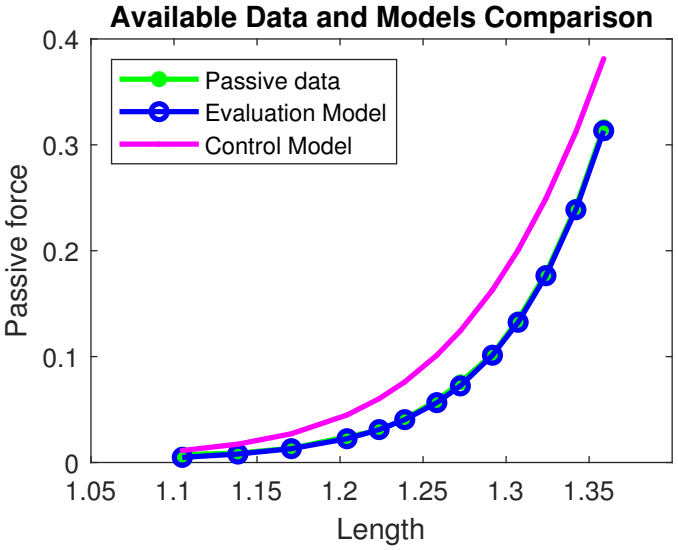

Figure 7: Passive force comparisons among the available data in green, the Evaluation model in blue, and the control model in magenta. The residual values for the Evaluation model has norm $|r_{EM}|_2 = 0.0077$ and for the Control model the norm is $|r_{CM}|_2 = 0.1706$

where α is the α-motoneuron excitation frequency and L is the muscle length. In order to obtain such a final model, we first designed an intermediate/evaluation model following Winters' considerations. Indeed, we exploited the negative passive term introduced in [10] to obtain the rest length values for the different excitation frequencies. This step allows us to then construct and fit the parameters of the final/control model (7).

4.1. Evaluation Model

In order to construct the intermediate/evaluation model we consider the isometric force as divided in active F_L and passive F_p terms, as exploited in [10]:

$$F_{ISO}(\alpha, L) = F_L(\alpha, L) + F_p(L).$$

Inspired, then, by the modelling approach in [11] we describe the active force curves as Gaussian functions with mean value μ and standard deviation σ and amplitude A as a function of the excitation frequency α, as shown in (4.1).

$$\begin{aligned} F_{\text{active}} &= Ae^{-\left(\frac{L-\mu}{\sigma}\right)^2} \\ A &= \frac{c_{11}\alpha^2 + c_{12}\alpha + c_{13}}{\alpha^2 + c_{14}\alpha + c_{15}} \\ \mu &= c_{21}e^{c_{22}\alpha} + c_{23}e^{c_{24}\alpha} \\ \sigma &= c_{31} + c_{32}\cos(c_{34}\alpha) + c_{33}\sin(c_{34}\alpha) \end{aligned}$$

By running a curve fitting algorithm we are able to fit the active isometric force with a very good order of approximation, i.e. the standard euclidean norm of the residual vector is $|r|_2 = 0.051$, where r is the stack of the differences between the available force data and the related value of the proposed model. In Fig.6 we plotted the active force comparison between the available data from [11] and the intermediate model estimation. The identified coefficients are reported in Tab.1.

Table 1: Parameters of Evaluation Model active force.

i	c_{i1}	c_{i2}	c_{i3}	c_{i4}	c_{i5}
1	1.134	0.723	0.0504	11.3297	643.259
2	0.574	−0.0211	0.8477	0.0008	n.a.
3	0.4518	−0.01704	−0.1235	0.04898	n.a.

Exploiting the data available in [10] and their negative passive terms considerations we propose a unified continuous model of the passive force term exploiting a sigmoidal and exponential function

$$F_p(L) = f_1 + \frac{f_2 - f_1}{1 + 10^{f_3(f_4 - L)}} + f_5 e^{f_6 L} \tag{8}$$

were the coefficient values f_i, for $i = 0, \ldots, 6$, can be found in Tab.2. The sigmoidal behaviour in the passive term, see Fig.10, does not have an experimental data correspondence but provides a plausible description of the physical limit of every elastic material, i.e. beyond the 'boundary' length value the solicited fibres start to break. Then the total isometric force will result from the saturation at 0 of all negative terms, as in

Table 2: Parameters of Evaluation Model passive force.

f_1	f_2	f_3	f_4	f_5	f_6
0.00381	2.16582	8.16634	1.45388	−7.32	−7.4

$$F_{ISO}(\alpha, L) = \begin{cases} F_{passive}(L) + F_L(\alpha, L) \\ 0, \quad F_{Iso} \leq 0 \end{cases} \tag{9}$$

4.2. Control Model

Due to the high complexity of the intermediate/evaluation model (9), and in order to make the force relationship more in-

tuitive from a physical standpoint, we exploited the intermediate model to find the rest length points and then the equivalent stiffness values. These data were fundamental to then fit the rest length $L_0(\alpha)$ and stiffness $K(\alpha,L)$ functions' parameters in terms of the α and L, so to construct the final/control model. Thus, the isometric force function is given by (7), reported here for completeness,

$$F_{ISO}(\alpha,L) = K(\alpha,L)\,(L - L_0(\alpha)) \tag{10}$$

where both L_0 and K are taken as polynomial functions in α and L

$$\begin{aligned} L_0(\alpha) &= \ell_1\alpha^2 + \ell_2\alpha + \ell_3 \\ K(\alpha,L) &= k_1(L)\alpha^3 + k_2(L)\alpha^2 + k_3(L)\alpha + k_4(L) \end{aligned} \tag{11}$$

where the $k_i(\cdot)$, $i = 1\ldots4$, a polynomial functions in α

$$\begin{aligned} k_i(\alpha) = k_{i1}\alpha^6 + k_{i2}\alpha^5 + k_{i3}\alpha^4 + k_{i4}\alpha^3 + k_{i5}\alpha^2 \\ + k_{i6}\alpha + k_{i7}. \end{aligned} \tag{12}$$

The relative coefficients values are reported in Tables 3 and 4, respectively.

Table 3: Parameters of Control Model rest legth.

ℓ_1	ℓ_2	ℓ_3
$6.794\cdot10^{-5}$	-0.01271	1

We also report in Fig.8 a comparison between the stiffness surface $K(\alpha,L)$ and the constructed point from the evaluation model with respect to the α and L values.

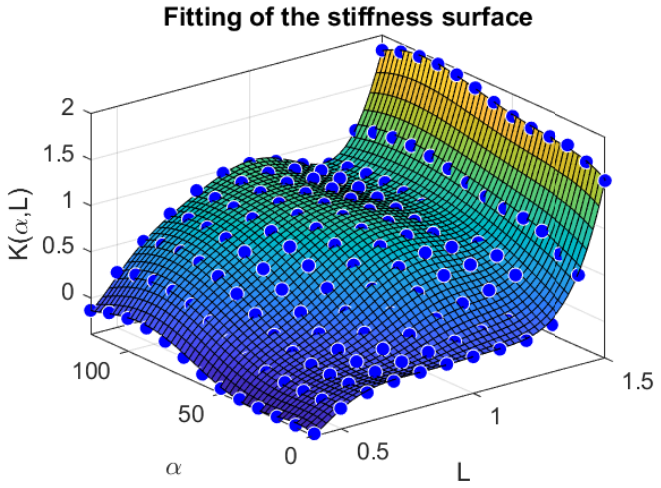

Figure 8: Fitting of the stiffness $K(\alpha,L)$ surface with respect to α and L

The model provides a good approximation of the Evaluation Model and, as a consequence, of the experimental data, as it is shown in Fig.9. Moreover, the new model of the total force gives a good approximation of the Evaluation one in the range $[0.4, 1.5]L_o$, see Fig.10. This model still provides a good level of approximation of the available data. Indeed, the residual vector norm is quite small $|r|_2 = 0.18$, especially for $L < 1.5$. Since

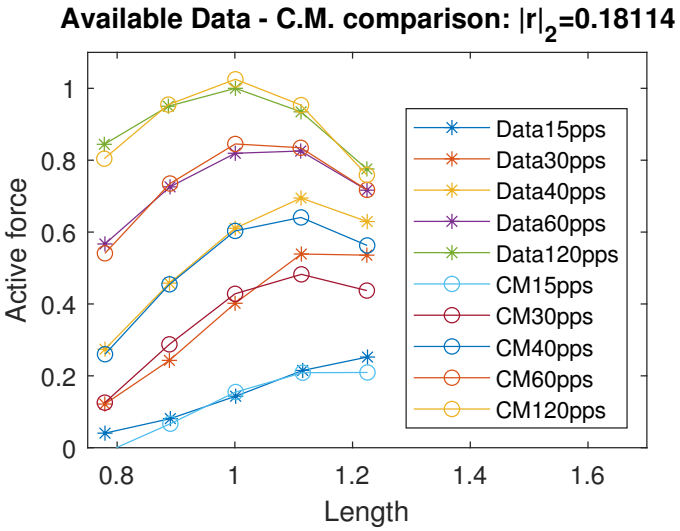

Figure 9: Data comparison with Spring Model. r indicates the residuals vector.

higher length values are usually not admissible in standard motions due to the mechanical limitation of biological joints, one can exploit the proposed control model in scenarios involving such standard motions.

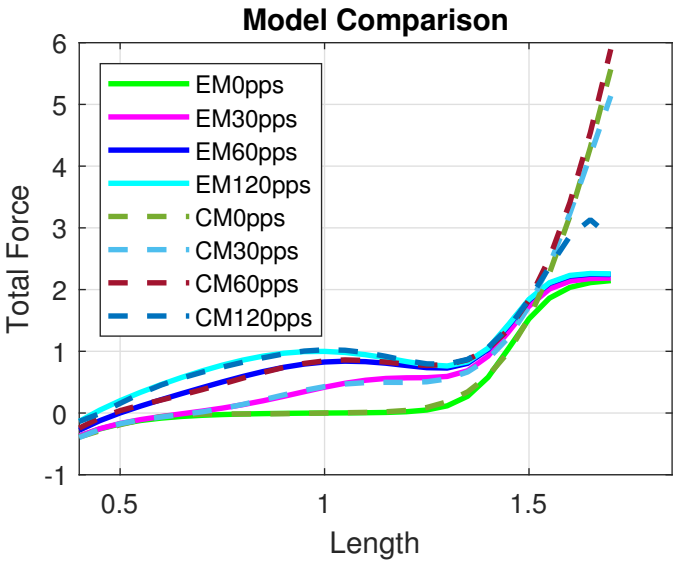

Figure 10: Comparison between the Evalution and the Control Model for different excitation frequencies, i.e. $\alpha \in 0, 30, 60, 120$ pps.

5. Sensors modelling

In this section, we talk about the dynamic modelling of the organs available as sensors. They measure the muscle length and velocity, along with the applied force at the tendon level. Respectively, these organs are spindle II and Ia, and Ib (also called Golgi Tendon Organs). For a model of the last ones we refer the reader to the works [41] and [23].

Table 4: Parameters of Control Model stiffness.

i	k_{i1}	k_{i2}	k_{i3}	k_{i4}	k_{i5}	k_{i6}	k_{i7}
1	−0.00041	0.0025	−0.0061	0.00763	−0.0052	0.0018	−0.00026
2	0.0586	−0.352	0.8444	−1.0277	0.6697	−0.2257	0.0319
3	−1.67504	9.829	−22.692	25.896	−15.268	4.5087	−0.5351
4	−40.977	244.666	−569.9335	664.1912	−405.645	120.853	−13.045

5.1. Spindles Ia and II

Ia- and II- spindles neuronal activities are correlated to the length and rate of change of the muscle fibres contractions. Along with each of the Spindles, we find active elements, i.e. the γ-motoneurons whose excitation frequency modifies the spindles' characteristics. In particular, such modulation can be interpreted as an increasing of sensing precision from the Spindles organs, despite the noise amplification drawback. We can generally distinguish between static, γ_s, and dynamic, γ_d, γ-motoneurons. In the modelling we only consider the effects of the γ_d-motoneurons on the spindles spiking frequency due to the lack of available data.

It is worth noticing in Fig.11b that in Spindle-Ia during negative velocities transient the output of the sensor saturates at zero while it is not clear what happens for Spindle-II due to the end of γ_s-excitation during the same part of the trajectory (negative velocities transients).

To construct the model of the sensors, we first find the static behaviour of the sensors' outputs, we make an analysis on the slopes as similarly done in [24].

We now first show the hybrid dynamical model found for the Spindle-Ia and then the one of the Spindle-II.

5.1.1. Spindle-Ia

We considered an Hybrid dynamical model and is given by

$$
\begin{aligned}
C_{Ia}: &\begin{cases} \dot{x}_{Ia} = p_{Ia}\left(K_{L_{Ia}} L - x_{Ia}\right) \\ \dot{p}_{Ia} = 0 \\ \dot{K}_{L_{Ia}} = 0 \\ y_{Ia} = \mathrm{sat}_0\left(x_{Ia} + K_{\gamma_{Ia}}\gamma_{Ia} + K_{\dot{L}_{Ia}}\dot{L}\right) \end{cases} \\
D_{Ia}: &\begin{cases} (\forall X_{Ia} \in D_{Ia1}) & K^+_{L_{Ia}} = 0,\ p^+_{Ia} = \bar{p}_{Ia} \\ (\forall X_{Ia} \in D_{Ia2}) & K^+_{L_{Ia}} = \bar{K}_{L_{Ia}},\ p^+_{Ia} = \bar{p}_{Ia} \\ (\forall X_{Ia} \in D_{Ia3}) & K^+_{L_{Ia}} = 0,\ p^+_{Ia} = \underline{p}_{Ia} \\ (\forall X_{Ia} \in D_{Ia}) & x^+_{Ia} = x_{Ia},\ y^+_{Ia} = y_{Ia} \end{cases}
\end{aligned}
\tag{13}
$$

where x_{Ia} is the filter state, y_{Ia} is its output, the function sat_0 is the function that saturates at zero negative values, p_{Ia} is the filter pole, $K_{L_{Ia}}$, $K_{V_{Ia}}$ and $K_{\gamma_{Ia}}$ are the static gains for the muscle length, velocity and the excitation state of the γ_d-motoneuron; in this case, L, V and γ_{Ia} are the muscle length, velocity and the excitation state of γ_d-motoneuron and are considered as system inputs. Then X_{Ia} is the vector collecting the state, inputs and output of the system. The flow set $C_{Ia} = \mathbb{R}^3 \backslash D_{Ia}$ while the jump set is $D_{Ia} = D_{Ia1} \cup D_{Ia2} \cup D_{Ia3}$, where

$$D_{Ia1} = \{X_{Ia} : \dot{L} < 0 \,\&\, (K_{L_{Ia}} \neq 0 || p_{Ia} \neq \bar{p}_{Ia})\},$$

$$D_{Ia2} = \{X_{Ia} : \dot{L} > 0 \,\&\, (K_{L_{Ia}} \neq \bar{K}_{L_{Ia}} || p_{Ia} \neq \bar{p}_{Ia})\},$$

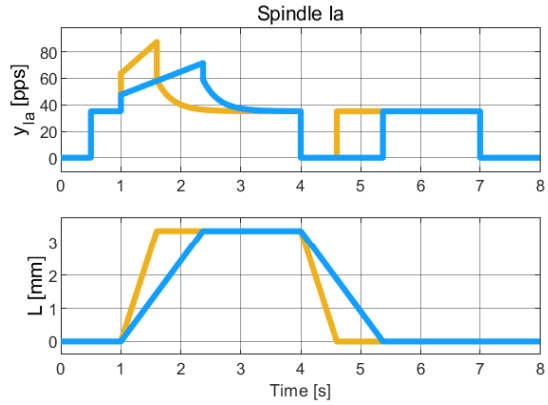

(a) Spindle Ia simulation with hybrid dynamical system

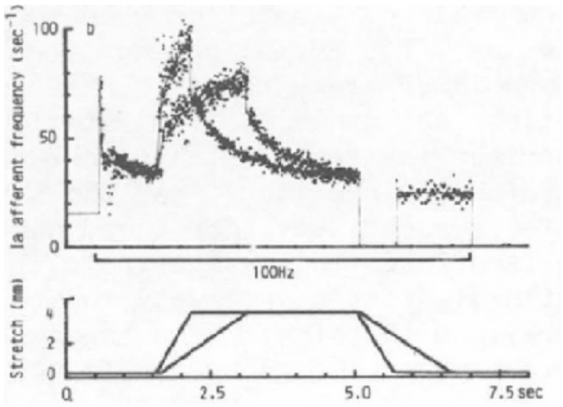

(b) Experimental Data of Spindle Ia from [21][Ch.19]

Figure 11: Spindle Ia Model output with experimental data in [21][Ch.19] comparison

$$D_{Ia3} = \{X_{Ia} : \dot{L} = 0 \,\&\, (K_{L_{Ia}} \neq 0 || p_{Ia} \neq \underline{p}_{Ia})\}.$$

In Fig.11 we compare the output of the dynamical system (13) with the available experimental data. The identified parameters are all gathered in Tab.5.

Table 5: Parameters of spindle Ia model.

$\bar{p}_{Ia}$	$\underline{p}_{Ia}$	$\bar{K}_{L_{Ia}}$	$K_{\dot{L}_{Ia}}$	$K_{\gamma_{Ia}}$
85	3.858	7.15	5.15	0.3514

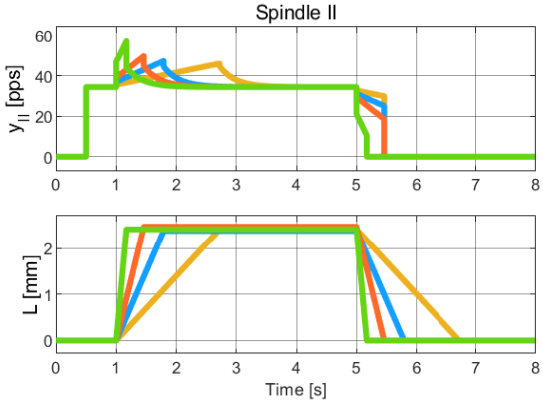

(a) Spindle II simulation with hybrid dynamical system

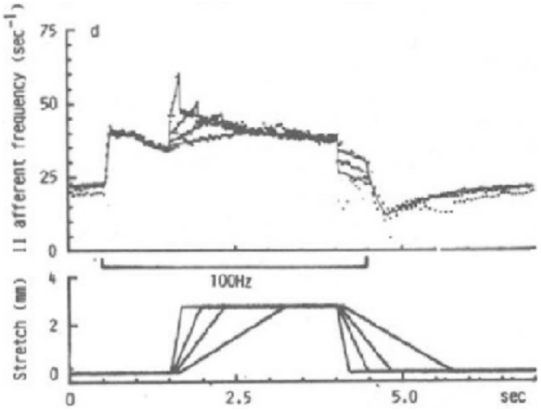

(b) Experimental Data of Spindle II in [21][Ch.19]

Figure 12: Spindle II Model output with experimental data in [21][Ch.19] comparison

5.1.2. Spindle-II

Also for this sensing system a Hybrid dynamical model and is given, similarly, by

$$C_{II}: \begin{cases} \dot{x}_{II} = p_{II}\left(\xi_{L_{II}} K_{L_{II}} L - x_{II}\right) \\ \dot{p}_{II} = 0 \\ \dot{\xi}_{L_{II}} = 0 \\ y_{II} = \mathrm{sat}_0\left[x_{II} + K_{\gamma_{II}}\gamma_{II} + K_{\dot{L}_{II}}\dot{L} + \right. \\ \qquad \left.\left(1-\xi_{L_{II}}\right)K_{L_{II}}\left(L-\bar{L}\right)\right] \end{cases} \tag{14}$$

$$D_{II}: \begin{cases} (\forall X_{II} \in D_{II1}) & \xi^+_{L_{II}} = 0,\ p^+_{II} = \bar{p}_{II} \\ (\forall X_{II} \in D_{II2}) & \xi^+_{L_{II}} = 1,\ p^+_{II} = \bar{p}_{II} \\ (\forall X_{II} \in D_{II3}) & \xi^+_{L_{II}} = 0,\ p^+_{II} = \underline{p}_{II} \\ (\forall X_{II} \in D_{II}) & x^+_{II} = x_{II},\ y^+_{II} = y_{II} \end{cases}$$

where x_{II} is the filter state, y_{II} is system output, the function sat_0 is the function that saturates at zero any negative argument, p_{II} is the filter pole, $K_{L_{II}}$, $K_{V_{II}}$ and $K_{\gamma_{II}}$ are the static gains for the muscle length, velocity and the excitation state of γ_d-motoneuron; in this case, L, V and γ_{II} are the muscle length, velocity and the excitation state of γ_d-motoneuron and are considered as system inputs. Then X_{II} is the vector collecting the state, inputs and output of the system. The flow set $C_{II} = \mathbb{R}^3 \backslash D_{II}$ while the jump set is $D_{II} = D_{II1} \cup D_{II2} \cup D_{II3}$, where

$$D_{II1} = \{X_{II} : \dot{L} < 0 \,\&\, (\xi_{L_{II}} \neq 0 || p_{II} \neq \bar{p}_{II})\},$$
$$D_{II2} = \{X_{II} : \dot{L} > 0 \,\&\, (\xi_{L_{II}} \neq 1 || p_{II} \neq \bar{p}_{II})\},$$
$$D_{II3} = \{X_{II} : \dot{L} = 0 \,\&\, (\xi_{L_{II}} \neq 0 || p_{II} \neq \underline{p}_{II})\}.$$

In Fig.12 we make a comparison between the output of the dynamical system (14) with the experimental available. The identified parameters are all gathered in Tab.5.

Table 6: Parameters of spindle II model.

$\bar{p}_{II}$	$\underline{p}_{II}$	$\bar{K}_{L_{II}}$	$K_{\dot{L}_{II}}$	$K_{\gamma_{II}}$	$\bar{L}$
85	2.858	4.334	0.9184	0.343	2.5

6. Conclusions and future works

In this work, we dealt with the modelling of muscle force considering the passive and active components of the isometric force. We first provided a brief overview of the model available in the literature and then show two models, an Evaluation and a Control one. The first one is more complex and precise than the second but does not add more concerning the available model in the literature. On the other hand, it allowed us to construct a set of data that have been useful for the identification of the second model parameters. The latter (the Control model) becomes easier to manage, although less precise than the intermediate one, and gives a physical intuition about the muscle behaviour. Indeed, it describes such muscular behaviour as a controllable non-linear spring with controllable (variable) stiffness K and rest length L_0.

We furthermore provide a Hybrid dynamical model formulation of the spindles organs that act as muscle length and velocity sensors for the Central Nervous System.

Future works concern the development of the muscle characteristic depending on the velocity of shortening and lengthening of the muscle fibres, so to provide a more complete model, and then analyse this new model in a control scenario involving joints with antagonist actuation.

References

[1] R. L. Lieber, Skeletal muscle structure, function, and plasticity, Lippincott Williams & Wilkins, 2002.

[2] W. R. Frontera, J. Ochala, Skeletal muscle: a brief review of structure and function, Calcified tissue international 96 (3) (2015) 183–195.

[3] H. L. Sweeney, D. W. Hammers, Muscle contraction, Cold Spring Harbor perspectives in biology 10 (2) (2018) a023200.

[4] I. Boyd, The isolated mammalian muscle spindle, Trends in neurosciences 3 (11) (1980) 258–265.

[5] A. V. Hill, The heat of shortening and the dynamic constants of muscle, Proceedings of the Royal Society of London. Series B-Biological Sciences 126 (843) (1938) 136–195.

[6] A. F. Huxley, Muscle structure and theories of contraction, Prog. Biophys. Biophys. Chem 7 (1957) 255–318.

[7] A. Gordon, A. F. Huxley, F. Julian, The variation in isometric tension with sarcomere length in vertebrate muscle fibres, The Journal of physiology 184 (1) (1966) 170–192.

[8] D. T. McRuer, R. E. Magdaleno, G. P. Moore, A neuromuscular actuation system model, IEEE Transactions on Man-Machine Systems 9 (3) (1968) 61–71.

[9] J. M. Winters, L. Stark, Analysis of fundamental human movement patterns through the use of in-depth antagonistic muscle models, IEEE transactions on biomedical engineering (10) (1985) 826–839.

[10] J. M. Winters, An improved muscle-reflex actuator for use in large-scale neuromusculoskeletal models, Annals of biomedical engineering 23 (4) (1995) 359–374.

[11] I. E. Brown, E. J. Cheng, G. E. Loeb, Measured and modeled properties of mammalian skeletal muscle. ii. the effectsof stimulus frequency on force-length and force-velocity relationships, Journal of Muscle Research & Cell Motility 20 (7) (1999) 627–643.

[12] G. Joyce, P. Rack, D. Westbury, The mechanical properties of cat soleus muscle during controlled lengthening and shortening movements, The Journal of physiology 204 (2) (1969) 461–474.

[13] P. M. Rack, D. Westbury, The effects of length and stimulus rate on tension in the isometric cat soleus muscle, The Journal of physiology 204 (2) (1969) 443–460.

[14] J. M. Winters, Hill-based muscle models: a systems engineering perspective, in: Multiple muscle systems, Springer, 1990, pp. 69–93.

[15] F. C. Van der Helm, L. A. Rozendaal, Musculoskeletal systems with intrinsic and proprioceptive feedback, in: Biomechanics and neural control of posture and movement, Springer, 2000, pp. 164–174.

[16] N. Hogan, Adaptive control of mechanical impedance by coactivation of antagonist muscles, IEEE Transactions on automatic control 29 (8) (1984) 681–690.

[17] I. E. Brown, G. E. Loeb, A reductionist approach to creating and using neuromusculoskeletal models, in: Biomechanics and neural control of posture and movement, Springer, 2000, pp. 148–163.

[18] J. McIntyre, J.-J. E. Slotine, Does the brain make waves to improve stability?, Brain research bulletin 75 (6) (2008) 717–722.

[19] J. M. Wakeling, S. S. Lee, A. S. Arnold, M. de Boef Miara, A. A. Biewener, A muscle's force depends on the recruitment patterns of its fibers, Annals of biomedical engineering 40 (8) (2012) 1708–1720.

[20] I. Boyd, P. Murphy, V. Moss, Analysis of primary and secondary afferent responses to stretch during activation of the dynamic bag 1 fibre or the static bag 2 fibre in cat muscle spindles, in: The muscle spindle, Springer, 1985, pp. 153–158.

[21] I. A. Boyd, M. H. Gladden, The muscle spindle, Springer, 1985.

[22] U. Windhorst, Muscle proprioceptive feedback and spinal networks, Brain research bulletin 73 (4-6) (2007) 155–202.

[23] M. P. Mileusnic, G. E. Loeb, Mathematical models of proprioceptors. ii. structure and function of the golgi tendon organ, Journal of neurophysiology 96 (4) (2006) 1789–1802.

[24] M. G. Maltenfort, R. Burke, Spindle model responsive to mixed fusimotor inputs and testable predictions of β feedback effects, Journal of neurophysiology 89 (5) (2003) 2797–2809.

[25] E. Schomburg, Spinal sensorimotor systems and their supraspinal control, Neuroscience research 7 (4) (1990) 265–340.

[26] P. B. Matthews, The human stretch reflex and the motor cortex, Trends in neurosciences 14 (3) (1991) 87–91.

[27] E. Jankowska, A neuronal system of movement control via muscle spindle secondaries., Progress in brain research 80 (1989) 299–303.

[28] M. M. Gassel, A critical review of evidence concerning long-loop reflexes excited by muscle afferents in man, Journal of Neurology, Neurosurgery & Psychiatry 33 (3) (1970) 358–362.

[29] R. M. Eccles, A. Lundberg, Supraspinal control of interneurones mediating spinal reflexes, The Journal of physiology 147 (3) (1959) 565–584.

[30] K. Iqbal, A. Roy, Stabilizing pid controllers for a single-link biomechanical model with position, velocity, and force feedback, J. Biomech. Eng. 126 (6) (2004) 838–843.

[31] D. A. Kistemaker, A. J. K. Van Soest, J. D. Wong, I. Kurtzer, P. L. Gribble, Control of position and movement is simplified by combined muscle spindle and golgi tendon organ feedback, Journal of neurophysiology 109 (4) (2013) 1126–1139.

[32] J. Nolte, The human brain, Mosby/Elsevier,, 1993.

[33] D. M. Wolpert, R. C. Miall, M. Kawato, Internal models in the cerebellum, Trends in cognitive sciences 2 (9) (1998) 338–347.

[34] O. Barak, Mark l. latash. neurophysiological basis of movement. human kinetics, champaign, 1998, Medicinski pregled 55 (5-6) (2002) 261–261.

[35] J. A. Kiernan, M. L. Barr, Barr's the human nervous system: an anatomical viewpoint, Lippincott Williams & Wilkins, 2009.

[36] M. A. Patestas, L. P. Gartner, A textbook of neuroanatomy, John Wiley & Sons, 2016.

[37] J. Huang, A. Isidori, L. Marconi, M. Mischiati, E. Sontag, W. Wonham, Internal models in control, biology and neuroscience, in: 2018 IEEE Conference on Decision and Control (CDC), IEEE, 2018, pp. 5370–5390.

[38] D. M. Wolpert, M. Kawato, Multiple paired forward and inverse models for motor control, Neural networks 11 (7-8) (1998) 1317–1329.

[39] M. Kawato, Internal models for motor control and trajectory planning, Current opinion in neurobiology 9 (6) (1999) 718–727.

[40] M. Mischiati, H.-T. Lin, P. Herold, E. Imler, R. Olberg, A. Leonardo, Internal models direct dragonfly interception steering, Nature 517 (7534) (2015) 333–338.

[41] M. P. Mileusnic, I. E. Brown, N. Lan, G. E. Loeb, Mathematical models of proprioceptors. i. control and transduction in the muscle spindle, Journal of neurophysiology 96 (4) (2006) 1772–1788.